

# Effect of Alloy Elements and Nitriding Conditions on Bending Fatigue Strength in Low C Alloy Steels.

Ryota Takao<sup>1</sup>, Naoki Fukuda<sup>1</sup>

<sup>1</sup> Aichi Steel Corporation, 1, Wanowari, Arao-machi, Tokai-shi, Aichi-ken 476-8666, JAPAN

The rotating bending fatigue strength was evaluated for nitrided low C alloy steels with a bainitic matrix structure, aiming for a fatigue strength higher than that of gas carburized JIS-SCM420 steel. The material compositions of the samples are based on that of SCM420, with a reduction of C content, addition of V content, and adjustment Cr and Al contents. In addition, in order to investigate the influence of the phase of compound layer, the nitriding potential  $K_N$  was varied so that the compound layer would be  $\epsilon$ -Fe<sub>3</sub>N or  $\gamma'$ -Fe<sub>4</sub>N phase. The nitriding treatment conditions were 853 K for 4 h, and the nitriding potential was set at two levels:  $K_N=2.0$  for the compound layer to be  $\epsilon$  phase, and  $K_N=0.3$  for the  $\gamma'$  phase. Surface hardness was higher in the order of Cr,Al-added steel, Cr-added steel, and base steel, with a corresponding increase in rotating bending fatigue strength. The same alloying effects on surface hardness and rotating bending fatigue strength are observed at  $K_N=0.3$  samples, mean while the bending fatigue strength was about 10% higher for  $K_N=0.3$  than for  $K_N=2.0$ . As a results, Cr,Al-added steel nitrided for  $K_N=0.3$  has about 20% higher rotating bending fatigue strength than SCM420 gas carburized.

**Keywords:** Nitriding, Alloy steel, Bending fatigue strength

## 1. Introduction

The properties required for automotive gears include excellent fatigue strength and quietness. A general-purpose material for gears is SCM420, a JIS steel. Since the required fatigue strength cannot be obtained without surface hardening treatment, the surface is usually hardened by gas carburizing to improve the strength. Gas carburizing improves the fatigue strength of components by heating them to the temperature at which austenite transformation occurs, diffusing the carbon, and then quenching them to make them hard martensite. However, this hardening causes distortion of the gear, resulting in reduced quietness during gear engaging. Therefore, we investigated the possibility of using gas nitriding, a surface hardening treatment below the austenite transformation temperature, to suppress distortion of the gear and achieve both excellent fatigue strength and quietness.

Gas nitriding treatment produces a compound layer of iron and nitrogen that is formed on the surface of the steel. This compound layer controls the nitriding potential and can generate the targeted crystalline phase ( $\epsilon$ -Fe<sub>3</sub>N phase or  $\gamma'$ -Fe<sub>4</sub>N phase)<sup>1,2</sup>. It has been reported that the bending fatigue strength is improved when this compound layer is the  $\gamma'$  phase<sup>3,4</sup>.

In this report, we report the results of the bending fatigue strength of a low C alloy steel with a bainitic matrix structure and a nitriding potential adjusted to produce an  $\epsilon$ -Fe<sub>3</sub>N or  $\gamma'$ -Fe<sub>4</sub>N compound layer, in order to improve fatigue strength at the gas carburizing ratio of SCM420, a JIS steel.

## 2. Experimental procedure

### 2.1 Test materials

The material composition of the specimens was based on the SCM420 with reduced C addition, V addition, and adjusted Cr and Al additions in order to improve nitriding properties such as surface hardness and hardened layer depth. The concept behind the composition adjustment is described below. For C, it is considered that the more the

amount of C added, the more stable the  $\epsilon$  phase is likely to become as the generating phase of the compound layer. Therefore, the amount of carbon content was reduced to facilitate the formation of the  $\gamma'$  phase. V is newly added because it precipitates as carbides and nitrides during nitriding, which can increase the hardness of the parts and may contribute to strength improvement. Cr and Al are precipitated as nitrides to improve surface hardness. Contents of Cr and Al were adjusted with the expectation that they would precipitate as nitrides and improve surface hardness. In this report, to verify the effects of Cr and Al additions on surface hardness improvement and bending fatigue strength, three steel grades were used as shown in Table 1: Base steel (Cr=0.5 mass%, called Base), material with Cr addition increased from 0.5 to 1.5 mass% in the base steel (called Cr-added steel or simply 1.5Cr), and material with 0.1 mass% of Al added (called Cr,Al-added steel or simply 1.5Cr-0.1Al). Furthermore, for the purpose of strength improvement, the matrix structure was set to bainite, and the amount of Mn added was adjusted to obtain this structure.

Table 1 Chemical compositions of test specimens (mass%).

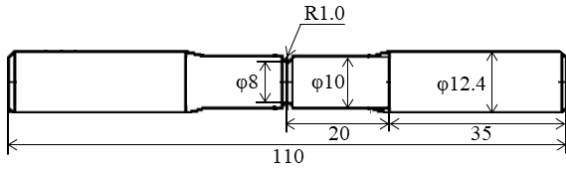
	C	Si	Mn	Cr	Mo	Al	V
Base	0.10	0.10	1.48	0.50	0.18	0.002	0.50
1.5Cr	0.10	0.10	1.02	1.51	0.18	0.006	0.50
1.5Cr-0.1Al	0.10	0.10	1.02	1.51	0.18	0.110	0.50

### 2.2 Preparation of test specimens

Three steel grades with the chemical compositions shown in Table 1 were melted and drawn into a round bar shape of  $\phi 15 \times 360$  mm. The bars were then heated at 1230°C for 1h and air cooled to a bainitic structure. It was roughly machined into the notched rotating bending fatigue specimen (notch: R=1.0mm, stress concentration factor:  $\alpha=1.78$ ) shown in Figure 1, and then nitrided. The nitriding was performed in an ammonia and hydrogen atmosphere at a treatment temperature of 853 K for 4 h. The nitriding potential was set at two levels:  $K_N = 2.0$  for the compound layer to be in the  $\epsilon$  phase and  $K_N = 0.3$  for the  $\gamma'$  phase. After the nitriding, the gripping part of the specimen was

machined to a finish and subjected to bending fatigue testing.

Figure 1 Geometry of bending fatigue test specimen.



### 2.3 Evaluation methods

The microstructure of the specimens before nitriding was observed by optical microscopy. For the specimens after nitriding, the formation phase of the compound layer was analyzed by EBSD, and measurement of hardness profile by a micro-Vickers hardness tester. Hardness distribution was measured at a load of 0.98 N at 0.05 mm depths from the surface in 0.05 mm intervals toward the interior. Fatigue tests were performed at room temperature, stress ratio  $R=-1$ , and 3600 rpm in an Ono-type rotating bending fatigue tester, and S-N diagrams were collected.

## 3. Experimental results

### 3.1 Material properties

Figure 2 shows the results of microstructural observation before nitriding by optical microscopy, and Figure 3 shows the results of analysis of the compound layer after nitriding by EBSD, both conducted on Cr-added steel as an example. Figure 2 shows that the structure before nitriding is mainly bainite. The image quality map in Figure 3 shows that after nitriding, a compound layer is formed on the topmost

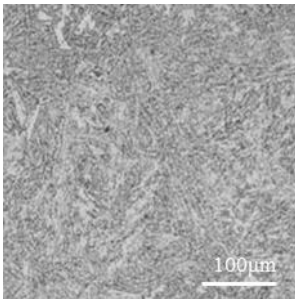


Figure 2 Microstructural observation before nitriding by optical microscopy at the Cr-added steel.

surface layer, and the bainite structure of the matrix phase is below the compound layer. Figure 3 also shows that the  $\epsilon$  phase is the mainly formed phase in the compound layer after nitridation at a nitridation potential of  $K_N=2.0$ , while the  $\gamma'$  phase is formed on the topmost surface at  $K_N=0.3$ . Figure 4 shows the results of hardness profile measurement. For each type of steel and each nitriding condition, there is a diffusion layer of nitrogen in which the hardness decreases gradually from the surface to the interior, and in the Base steel, the hardness decreases rapidly at around 0.3 mm and is about the same as that of the substrate. In the Cr-added and Cr,Al-added steels, the hardness decreased rapidly around 0.2 mm, and the hardness was about the same as that of the substrate. The near-surface hardness measured at the 0.05 mm depth was the highest for the Cr,Al added steel nitrided at a nitriding potential of  $K_N=2.0$ . When compared for each nitriding condition, the hardness was higher for Base, Cr-added steel, and Cr,Al-added steel, in that order. When compared for each type of steel, the specimens nitrided at  $K_N=0.3$  had lower hardness than

those nitrided at a nitriding potential of  $K_N=2.0$ .

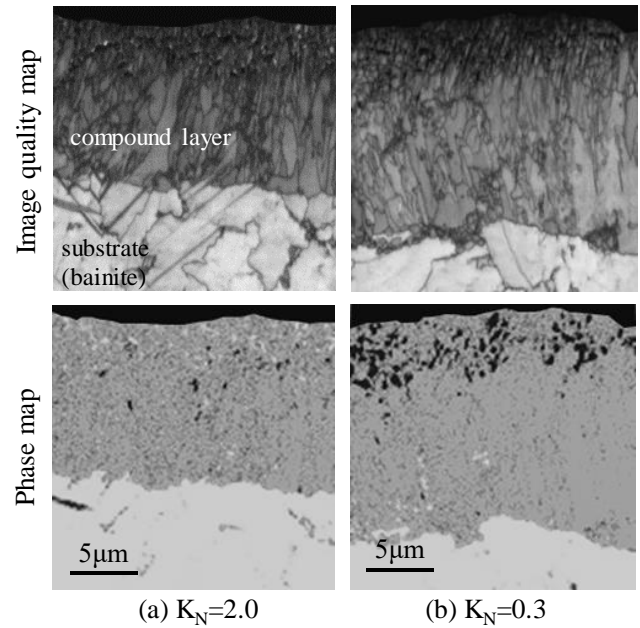


Figure 3 EBSD analysis result of the compound layer at the Cr-added steel.

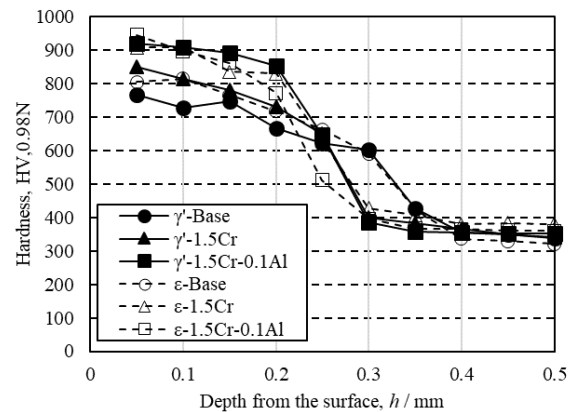


Figure 4 Hardness profile of test specimens.

### 3.2 Bending Fatigue Test

Figure 5 shows the results of the rotating bending fatigue test. When the fatigue strength was defined as the stress at which the specimen endured without fracture after  $10^7$  cycles of testing, the Cr,Al-added steel nitrided at nitriding potential  $K_N=0.3$  resulted in the highest fatigue strength. Comparing the results for each nitriding condition, the fatigue strength is higher in the order of Cr,Al-added steel, Cr-added steel, and Base steel. In addition, for each type of steel, the fatigue strength was higher for specimens nitrided at  $K_N=0.3$  than at nitriding potential  $K_N=2.0$ . Fracture surface observations after bending fatigue tests indicated that fracture occurred near the surface under many test conditions. In some cases, fracture originated from the grain boundary of large crystal grains at around 0.3 mm from the surface.

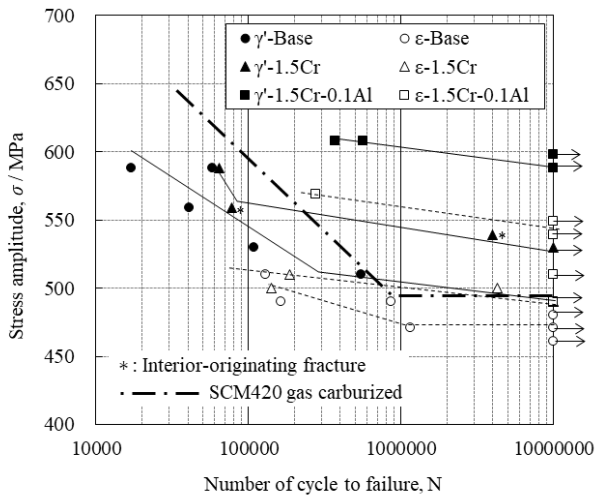


Figure 5 S-N diagrams measured by the rotating bending fatigue test.

#### 4. Discussion

As shown in Figure 4, regardless of the nitriding conditions, the hardness near the surface increases in the order of Cr,Al-added steel, Cr-added steel, and base steel, suggesting that the increase in the amount of Cr and Al addition increased the amount of nitride precipitation, which in turn increased hardness. As shown in Figure 5, the bending fatigue strength was also higher in the order of Cr,Al-added steel, Cr-added steel, and base steel, regardless of the nitriding condition, and the trend was similar to that of near-surface hardness. In addition, for each type of steel, the fatigue strength of the specimens nitrided at  $K_N=0.3$  was higher than that of the specimens at  $K_N=2.0$  although hardness at  $K_N=0.3$  is slightly lower than those at  $K_N=2.0$ .

As an exponential formula for fatigue strength,  $\sigma \cong 1.6HV$  is often used. Figure 6 shows the calculated local fatigue strength at each hardness measurement location from the surface. The local fatigue strength at 0.05mm is about 1230~1510 MPa but actual fatigue strength occurring at the surface is much lower. When residual stresses are taken into account, this difference is expected to be larger. If the fracture origin is at the surface, it is assumed that the compound layer is brittle and cracks occur at lower stresses,

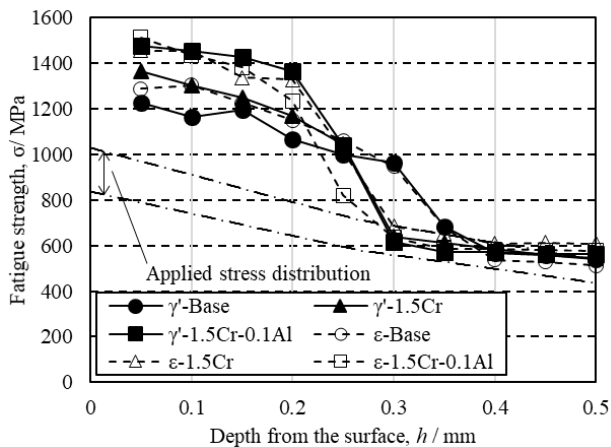


Figure 6 Distribution of calculated local fatigue strength and applied stress at actual fatigue strength.

which may be a factor in the strength loss. Enhancement of fatigue strength by the formation of the  $\gamma'$  phase is expected to be due to the improved toughness of the compound layer.

#### 5. Summary

In this report, bending fatigue strength of a low C alloy steel with bainite matrix was investigated by nitriding treatment in which the nitriding potential was adjusted so that  $\epsilon\text{-Fe}_3\text{N}$  or  $\gamma'\text{-Fe}_4\text{N}$  phase was formed in the compound layer, and the following results were obtained. (i) Addition of Cr and Al increased the hardness near the surface, which in turn increased the bending fatigue strength. (ii) The  $\gamma'$  phase of the compound layer increased the bending fatigue strength by about 10% for each type of steel. (iii) As a result, the rotating bending fatigue strength of the nitrided Cr and Al added steel with  $K_N=0.3$  was about 20% higher than that of the gas carburized SCM420.

#### 6. References

- 1) D. Liedtke, U. Baudis, J. Boßlet, U. Huchel, H. K. Westkamp, W. Lerche, and H. J. Spies: *Nitriding and Nitrocarburizing on Iron Materials*, AGNE Gijutsu Center, Tokyo, 2011.
- 2) Y. Hiraoka, Y. Watanabe: *Journal of the Japan Society for Heat Treatment* **55** (2015) 7-11.
- 3) A. Kobayashi, S. Maeda, H. Imataka, Y. Gyotoku, M. Yuya, Y. Shimizu, M. Kanayama: *Transactions of Society of Automotive Engineers of Japan* **45** (2014) 1153-1158.
- 4) Y. Hiraoka, A. Ishida, O. Umezawa: *Journal of the Japan Society for Heat Treatment* **52** (2017) 64-72.